Biochemistry and Biophysics Reports 12 (2017) 214–219

Contents lists available at ScienceDirect

Biochemistry and Biophysics Reports

journal homepage: www.elsevier.com/locate/bbrep

Novel elvitegravir nanoformulation approach to suppress the viral load in HIV-infected macrophages

Yuqing Gong, Pallabita Chowdhury, Narasimha M. Midde, Mohammad A. Rahman, Murali M. Yallapu*, Santosh Kumar*

Department of Pharmaceutical Sciences, College of Pharmacy, University of Tennessee Health Science Center, Memphis, TN 38163, USA

ARTICLE INFO

Keywords:
PLGA nanoparticles
Antiretroviral therapy
Elvitegravir
HIV
Monocytes
Drug delivery systems

ABSTRACT

Purpose: Monocytes serve as sanctuary sites for HIV-1 from which virus is difficult to be eliminated. Therefore, an effective viral suppression in monocytes is critical for effective antiretroviral therapy (ART). This study focuses on a new strategy using nanoformulation to optimize the efficacy of ART drugs in HIV-infected monocytes.
Methods: Poly(lactic-*co*-glycolic acid) (PLGA)-based elvitegravir nanoparticles (PLGA-EVG) were prepared by nano-precipitation technique. The physicochemical properties of PLGA-EVG were characterized using transmission electron microscopy, dynamic light scattering, and Fourier-transform infrared spectroscopy. Cellular uptake study was performed by fluorescence microscopy and flow cytometry. All in vitro experiments were performed by using HIV-infected monocytic cell lines U1 and HIV-infected primary macrophages. Elvitegravir quantification was performed using LC-MS/MS. HIV viral replication was assessed by using p24 ELISA.
Results: We developed a PLGA-EVG nanoparticle formulation with particle size of ~ 47 nm from transmission electron microscopy and zeta potential of ~ 6.74 mV from dynamic light scattering. These nanoparticles demonstrated a time- and concentration-dependent uptakes in monocytes. PLGA-EVG formulation showed a ~ 2 times higher intracellular internalization of EVG than control group (EVG alone). PLGA-EVG nanoparticles also demonstrated superior viral suppression over control for a prolonged period of time.
Conclusions: PLGA-based EVG nanoformulation increased the intracellular uptake of EVG, as well as enhanced viral suppression in HIV-infected macrophages, suggesting its potential for improved HIV treatment in monocytic cells.

1. Introduction

Monocyte/macrophage lineage cells express the CD4 receptor and chemokine coreceptors for entry of Human Immuno deficiency Virus-1 (HIV-1) [1]. Thus, they perform an important role of initial HIV-1 infection. Moreover, monocytes/macrophages are more resistant to HIV-induced apoptosis, and are a crucial reservoir for HIV-1 [2,3]. Antiretroviral therapy (ART) has notably improved the life of HIV-1 infected patients. However, it is difficult to maintain therapeutic levels of ART drugs in monocytes, because drug efflux transporters, including p-glycoprotein (P-gp) and drug metabolic enzyme cytochrome P450 (CYP) 3A4 are expressed in these cells [4–6]. ART drugs, especially protease inhibitors show a 2–10 fold lower efficacy in monocytes than in T-lymphocytes [7]. Thus a new strategy to improve the bioavailability and efficacy of the ART drugs in monocytes/macrophages is highly desirable.

Nanoparticles have been used as drug delivery vehicles in research for many diseases [8–11]. Delivery of nanoparticle mediated therapeutics at the intracellular site of action is more efficient than individual molecules alone. Therefore, nanoparticles could be used as effective transportation and delivery systems in monocytes, and can bypass P-gp and CYP3A4 [12]. Therapeutic drugs can be encapsulated in the core of nanoparticles to be delivered specifically into HIV-infected monocytes thus achieving targeted therapy. In addition, drugs in nanoparticles have the ability to cross the blood-brain barrier (BBB) and suppress the HIV-1 from the CNS reservoirs [13,14]. Unfortunately, such nanoparticle approaches have not been well developed for HIV applications.

Elvitegravir (EVG), an integrase inhibitor, is the newest class of ART drug and is used as the first line therapy for the treatment of HIV infection [15]. EVG is predominately metabolized through the CYP3A4 pathway in the liver and perhaps also in the monocytic cells [16,17]. We selected EVG as the therapeutic molecule in our nanoformulation because EVG provides a more favorable safety profile than other ART

* Corresponding authors.
E-mail addresses: myallapu@uthsc.edu (M.M. Yallapu), ksantosh@uthsc.edu (S. Kumar).

http://dx.doi.org/10.1016/j.bbrep.2017.10.005
Received 18 September 2017; Accepted 16 October 2017
Available online 15 November 2017

drugs [18] and nano-formulated EVG may have the ability to bypass metabolic enzymes [19]. Therefore, the main objective of this study is to develop an EVG nanoformulation that shows increased efficacy in monocytic cells.

2. Material and methods

2.1. Chemicals and reagents

Elvitegravir was purchased from Toronto Research Chemicals Inc. (Ontario, Canada). Poly(D, L-lactide-*co*-glycolide) (PLGA) (50:50 lactide-glycolide ratio, Mw: 31,000–50,000, ester terminated) was purchased from Birmingham Polymers (Pelham, AL, USA). Other chemicals; poly(vinyl alcohol) (PVA) (363138, 30,000–70,000), poly(L-lysine) (PLL) (M.W. 30,000–70,000), pluronic F-68 (F-68) (P1300, MW:8350), Coumarin-6 (442631, MW:350.43), Phorbol-12-myristate-13 acetate (P8139), and acetone (650501) were purchased from Sigma-Aldrich (St. Louis, MO). Roswell Park Memorial Institute (RPMI) 1640 media was bought from Corning Inc (Tewksbury, MA). Fetal bovine serum (FBS) was obtained from Atlanta biologicals (Atlanta, GA). L-glutamine, and penicillin-streptomycin solution were purchased from Fisher Scientific (Pittsburgh, PA). Constitutively HIV-infected (U1) cell lines were obtained from NIH AIDS Reagent program (Germantown, MD). De-identified human blood, upon approval from Institutional Review Board (IRB), UTHSC, was obtained from interstate blood bank Inc. (Memphis, TN). The recombinant Human IL-2 and recombinant Human macrophage colony stimulating factor (M-CSF) were bought from PeproTech (Rocky Hill, NJ). HPLC grade acetonitrile and formic acid from Sigma-Aldrich (St. Louis, MO) were used in preparation of mobile phase. P24 ELISA kit (801111) was purchased from ZeptoMetrix Corp (Buffalo, NY).

2.2. Preparation of PLGA-based Elvitegravir nanoparticles

PLGA-based EVG nanoparticle (PLGA-EVG) formulation and control PLGA were prepared by nano-precipitation technique as described [20]. In brief, PLGA (45 mg) and EVG (4 mg) were dissolved in 4 mL of acetone to obtain PLGA-EVG uniform solution. This PLGA-EVG solution was added dropwise into 10 mL of 1% PVA-aqueous solution on a magnetic stir plate at 400 rpm. After 3 h, 10 mg of PLL was dissolved in 1 mL water, and 50 mg of pluronic polymer F-68 was dissolved in 4 mL water. PLL and F-68 solutions were added to the nanoparticle suspension and stirred at room temperature for ~ 24 h to evaporate acetone completely. The un-uniform and larger aggregates of PLGA, PLGA-EVG, PVA, and PLL ingredients were removed by centrifugation at 1000 rpm for 10 min. The finer and uniform PLGA-EVG nanoparticle formulation was stored at 4 °C until further use.

2.3. Characterization of PLGA-based Elvitegravir nanoparticles

The average particle size and zeta potential of the prepared PLGA-EVG nanoparticles were determined by the dynamic light scattering (DLS) using Zetasizer (Nano ZS, Malvern Instruments, Malvern, UK). The morphology of PLGA-EVG nanoparticles was confirmed by transmission electron microscope (TEM) (JEOL-2000EX, Tokyo, Japan). For the DLS measurements, freshly prepared PLGA-EVG nanoparticles suspension was diluted to 1 mg/mL with distilled water and probe sonicated (VirSonic Ultrasonic Cell Disrupter 100, VirTis) for 30 s. Particle size measurements were performed in water for 3 min at 25 °C. Zeta potential measurement was done upon diluting the suspensions to 1 mg/mL with 1 X phosphate-buffered saline (PBS). To study the morphology of nanoparticles, 20 μL of the 1 mg/mL of PLGA-EVG was carefully placed on the shiny side of the 200 mesh standard TEM grid (Electron Microscopy Sciences, PA, USA). Uranyl acetate solution (2%; w/v) was used to stain the nanoparticles for achieving positive contrast under TEM. To acquire the FTIR spectral data of formulation(s), samples were lyophilized to obtain dry solid powder using a Labconco Freeze Dry System (− 48 °C 133 × 10–3 m Bar; Labconco, Kansas City, MO, USA). Fourier transform infrared (FTIR) spectra were obtained on the Universal ATR sampling Accessory plate using a Spectrum 100 FTIR spectrophotometer (Waltham, MA) for drug encapsulation. The samples were placed on the tip of the ATR objective and spectra were obtained between 4000 and 650 cm^{-1}.

2.4. Cellular uptake of PLGA nanoformulation

Cellular uptake of nanoparticles were assessed by Accuri C6 Flow Cytometer (Accuri Cytometer Inc, Ann Arbor, MI), and images were taken by EVOS® FL Imaging System (AMF4300, Life Technologies, Carlsbad, CA). Monocytes (0.5×10^6) were cultured in a 6-well plate and allowed to attach overnight. Coumarin-6 dye was encapsulated in PLGA nanoparticles in a similar manner as drug loading in PLGA nanoparticles as described in Section 2.2. The particle size of Coumarin 6 loaded PLGA was measured by DLS. Coumarin-6 dye was used to track, locate, and measure the green fluorescence for semi-quantitative and qualitative cellular uptake. Cells were treated with 5 μg/mL of coumarin-6 equivalent PLGA nanoparticles at different time points (0.5, 1, 2, 3, 4 h) and at different concentrations of coumarin-6 (0.5, 1, 2.5, 5, 10 μg/mL) for 3 h. After the treatment and washing unlabeled cells, semi-quantitative and qualitative coumarin-6 uptake in PLGA nanoparticles were assessed by using flow cytometer with FL1 channel (488 excitation, blue laser, 530 ± 15 nm, FITC/GFP) and EVOS® FL Imaging System [20].

2.5. EVG quantification using LC-MS/MS

EVG or EVG in PLGA-EVG nanoparticles (drug encapsulation) was quantified using the LC-MS/MS method as described [17]. The LC-MS/MS system used was a liquid chromatography system (Shimadzu Corp., Kyoto, Japan) coupled to a tandem mass spectrometer (AB SCIEX, Triple Quad 5500, Framingham, MA). EVG standards and experimental samples were extracted by adding 3-volumes of cold acetonitrile, which contained 138 nM ritonavir (RTV) as an internal standard (IS). A 6 μL aliquot of extracted samples was injected into an Xterra® MS C18 column (125 Å, 3.5 μm, 4.6 mm × 50 mm; Waters, Milford) for separation. The mobile phase was consisted of (A) Water with 0.1% formic acid and (B) acetonitrile with 0.1% formic acid (v/v) at a flow rate of 1 mL/min. The gradient elution was as follows: 0–1.5 min, 50% B; 1.5–5.1 min, 60% B (v/v).

2.6. Cell culture and drug treatment

U1 cells were grown in RPMI media supplemented with 1% L-glutamine, 10% FBS, and penicillin-streptomycin solution. The cells were differentiated into macrophages using 100 nM phorbol-12-myristate-13 acetate (PMA) for 72 h. Differentiated cells were treated with native drug EVG at physiological concentration (1 μM), and nanoparticles of PLGA-EVG (1 μM). The EVG concentration in cell lysates was determined over a period of 0.1, 0.15, 0.5, 1, 3, 9, 24, 48, and 72 h by using the LC-MS/MS method described above.

Peripheral blood mononuclear cells (PBMCs) were collected from buffy coats and differentiated into primary macrophages as described [21]. The collected cells were infected with HIV-Ada strain at 20 ng/million. The HIV-infected primary macrophages were treated with vehicle (acetonitrile), EVG (1 μM), PLGA-EVG (1 μM), and blank PLGA nanoparticles for 10 days. Cell culture media samples were collected every 24 h to assess HIV p24 production by using p24 ELISA kit.

2.7. Statistical analysis

Area under the curve (AUC_{tot}) was calculated by the log-linear trapezoidal rule. The statistical significance between different

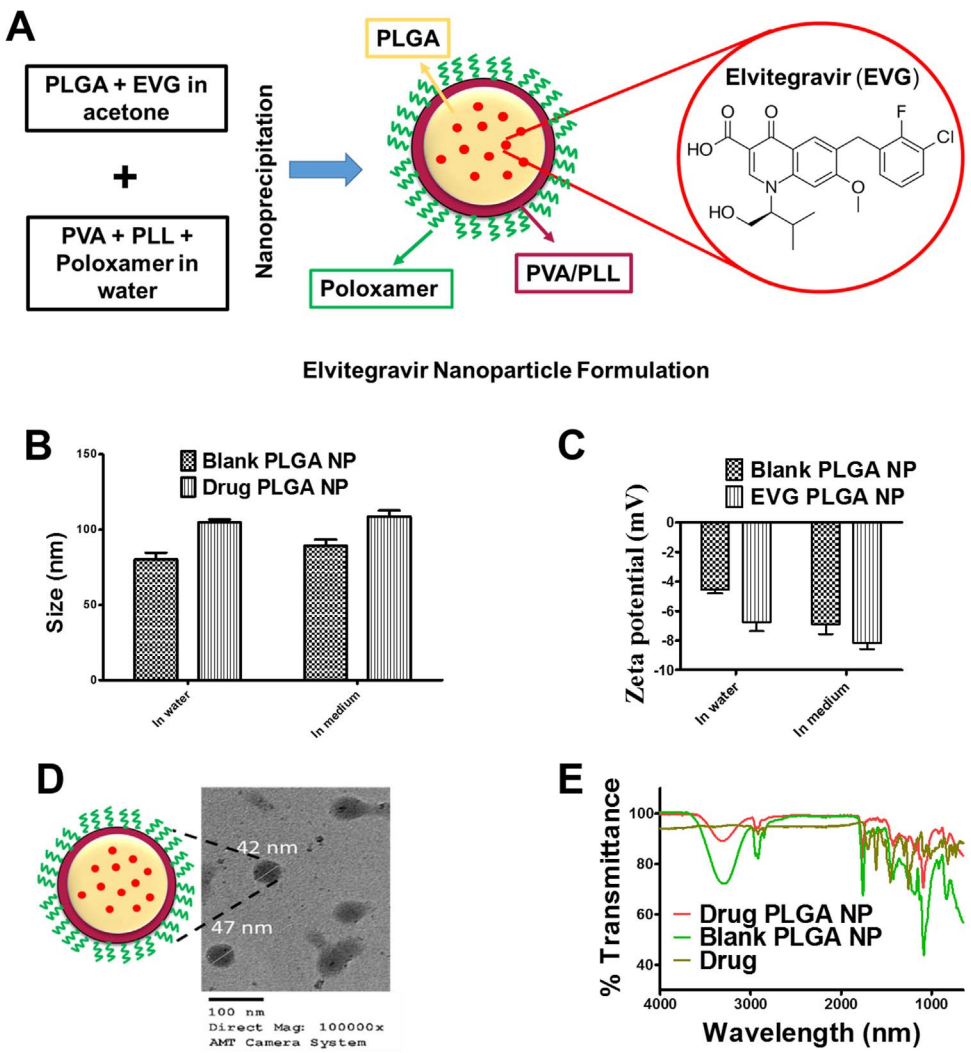

Fig. 1. PLGA-EVG nanoparticle formulation. **A.** A hypothetical structural representation of PLGA-EVG nanoparticle. **B.** DLS based particle size distribution. **C.** Zeta potential of PLGA-EVG nanoparticles. **D.** Morphology of PLGA-EVG nanoparticles as viewed under Transmission electron microscopy by using AMT camera at a direct magnification of 100,000x. Bar equals to 100 nm in TEM image. **E.** FT-IR spectral confirmation for drug encapsulation.

treatment and control groups was determined by using student *t*-test. All the statistical analyses were done by Prism 6 (GraphPad Software, La Jolla, CA). A p-value ≤ 0.05 among the treatment groups was considered significant.

3. Results

3.1. Characterization of PLGA-EVG

The goal of this study was to develop a nanoformulation for EVG that would increase its bioavailability and HIV-1 suppression in monocytic cells. The hypothetical single nanoparticle structure of PLGA-EVG is illustrated in Fig. 1A. PLGA forms the core for holding the native drug EVG and the layers of PVA and PLL were added to ensure better encapsulation efficiency of the EVG inside the nanoparticles. Pluronic F-68 (the PEO and PPO chains of F-68 polymer) was added to the formulation to maintain a stable suspension for therapeutic application. Blank PLGA nanoparticles when measured for particle size by DLS, demonstrated a size of 80 ± 4.43 nm and 89 ± 4.13 nm in water and cell culture media, respectively. To further confirm if drug loading to these particles causes any difference in size, we conducted DLS particle size measurement of the EVG loaded PLGA nanoparticles. Particle size distribution histogram confirms there is a slight increase in the size of drug loaded particles over blank nanoparticles, with EVG loaded PLGA nanoparticles size of 105 ± 1.79 nm in water and 109 ± 4.10 nm in cell culture medium (aqueous suspension) (Fig. 1B). The slight increase in size is considered low enough for active targeting to highly replicating HIV cells. To ensure that there is no significant difference in particle size of PLGA nanoparticles when introduced in in-vitro conditions we measured the particle size both in water and cell culture medium. We confirm that there is no change in size, and these nanoparticles can be used in vitro as well as in in-vivo models. DLS measurement confirms that the nanoparticle has a low zeta potential of ~ 6.74 mV (Fig. 1C). Particle size under TEM demonstrated 47 nm (Fig. 1D) suggesting PLGA-EVG has spherical morphology with 40–50 nm in both dry and wet particle size. The obtained particle size range and low positive zeta potential of PLGA-EVG nanoparticles are recommended and suitable for effective drug delivery purpose [22]. The FTIR analysis of EVG, PLGA-EVG, and blank PLGA nanoparticles are shown in Fig. 1E. A broad peak between 3600 and 3050 cm^{-1} was found in PLGA-EVG and blank PLGA nanoparticles due to the presence of hydroxyl groups of PLGA/F68 polymer [23,24]. The characteristic peak of EVG was observed in PLGA-EVG spectrum within specified range. The FTIR spectral analysis indicated that EVG was encapsulated in nanoparticles. EVG encapsulation was found to be ~ 92% (i.e., ~ 9.2 mg of EVG in 90 mg of PLGA NPs formulation).

3.2. Cellular uptake of PLGA nanoparticles

To ensure that the coumrin-6 loaded PLGA nanoparticles were of similar size as the parent moiety, we measured their size. Coumarin-6 PLGA nanoparticles were 85 ± 2.83 nm and 93 ± 2.90 nm in water and

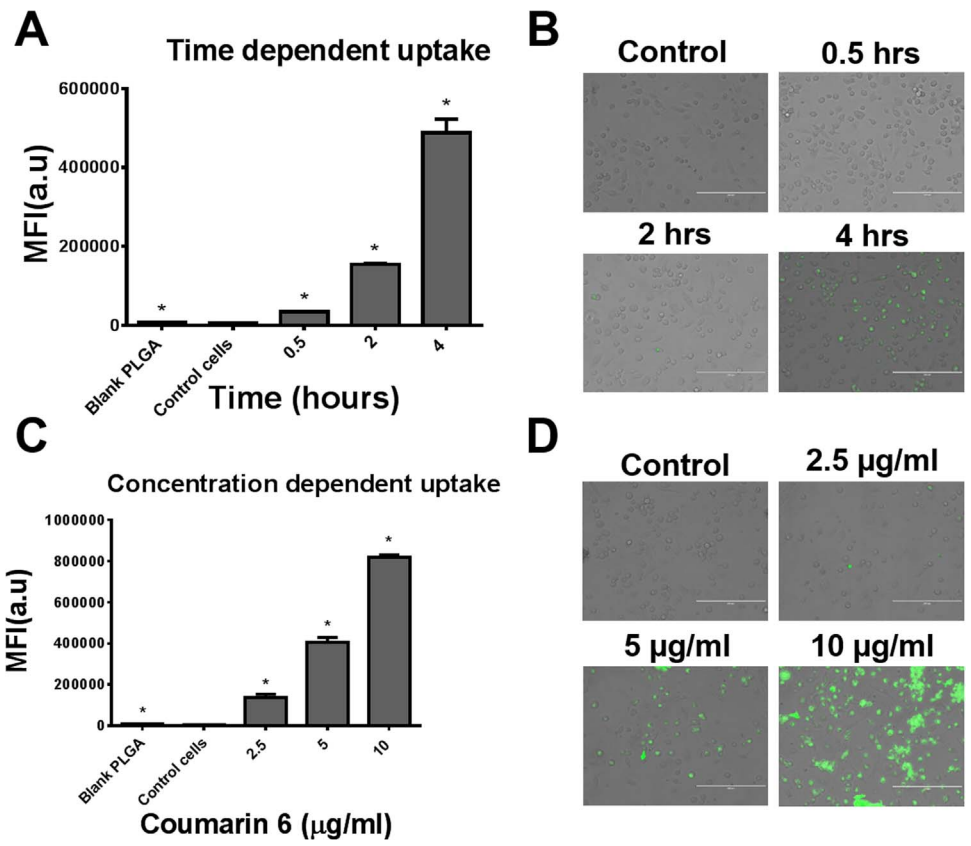

Fig. 2. Cellular uptake of nanoparticles. **A–B.** A time dependent cellular uptake of nanoparticles in monocytic cells. **C-D.** Dose dependent uptake of nanoparticles in monocytes. Qualitative uptake was confirmed by EVOS® FL Imaging System and semi-quantitative uptake was determined by Accuri C6 Flow Cytometer (Accuri Cytometer, Inc., Ann Arbor, MI, USA). Bar equals to 200 μm in microscopic images **B**, **D**. Mean ± SEM values were graphed from 3 independent experiments. $P \leq 0.05$ (*).

medium, respectively. The cellular uptake of PLGA nanoparticles in monocytes was presented in mean fluorescence intensity. A time-dependent increase in fluorescence intensity was observed (Fig. 2A–B), with the highest fluorescence after 4 h of exposure. Similarly, an increase in fluorescence intensity was observed with increasing concentrations of coumarin-6 (Fig. 2C–D). The highest fluorescence was observed in the cells treated with 10 μg/mL coumarin-6. Overall, the results showed that cellular uptake of PLGA nanoparticles followed time- and concentration-dependent profiles.

3.3. Intracellular EVG concentration

To evaluate the intracellular concentration of EVG, we performed an LCMS-MS method using RTV as internal control. EVG and RTV are eluted separately at approximately 3.27 and 2.72 min, respectively (Fig. 3A). The multiple reactions monitoring (MRM) transitions (*m/z*) Q1/Q3 selected for quantitative analyses were 447.9/343.8 for EVG and 721.3/296.1 for RTV. The standard curve was achieved over the range of 0.003–1 μM using linear regression ($r^2 = 0.99$) with a weighting factor of 1/x2 (Fig. 3A). We performed a short-term EVG/PLGA-EVG treatment in U1 cells and presented the EVG concentration as the percentage of initial EVG concentration (Fig. 3B). The results showed a consistent pattern of an ~ 2-fold increase in EVG concentration in PLGA-EVG nanoformulation than EVG alone (Fig. 3B). Furthermore, we calculated AUC_{tot} for EVG from both PLGA-EVG and EVG alone. AUC_{tot} of PLGA-EVG showed a significant (~ 2-fold) increase compared to EVG alone ($t = 9.340$, $p = 0.0113$, Fig. 3C). These results demonstrate that the EVG nanoformulation improves the intracellular delivery and drug retention in U1 cells.

3.4. Viral suppression of PLGA-EVG

To determine the efficacy of the viral suppression of EVG nanoformulation, HIV-infected primary macrophages were exposed to vehicle control, blank PLGA, EVG, and PLGA-EVG for 9 days. HIV p24 protein levels were measured every 24 h (Fig. 4A). Blank PLGA nanoformulation showed no effect on viral replication. EVG exposure to HIV-infected primary macrophages demonstrated a significant (~ 12%) decrease in viral replication on day 2 and day 3 ($p < 0.05$, compared to control). However, EVG showed lower efficacy on day 4 and no efficacy from day 5 to day 9 than the control. PLGA-EVG showed significantly higher efficacy for the viral suppression compared with EVG alone. Compared to control, PLGA-EVG exposure to HIV-infected primary macrophages demonstrated ~ 24% decrease in viral replication from day 2 to day 6 ($p < 0.05$).

4. Discussion

ART drugs, which are the substrates of P-gp and CYP3A4 require combination therapy and high dose for treatment [25]. These drugs also potentially develop resistance to HIV treatment [26]. Similar to protease inhibitors, EVG the most prescribed and newest drug, is also a substrate of CYP3A4 [16]. Thus, EVG is formulated with cobicistat, a CYP3A4 inhibitor, as a pharmacological enhancer, [17,27]. Therefore, it is desirable to develop a nanoparticle-based formulation for EVG that is likely to bypasses P-gp and CYP3A4 in the liver as well as in monocytic cells. With this regards, we developed a formulation of EVG encapsulated PLGA nanoparticles and investigated its efficacy on the viral suppression in HIV-infected macrophages. Our results showed that PLGA-EVG has higher intracellular EVG concentration, and relatively higher viral suppression for longer time than EVG alone in HIV-infected macrophages. This is the first report on EVG-NP based formulation that suppresses viral load in macrophages.

PLGA is an FDA-approved biodegradable polymer with minimal systemic toxicity for the use of drug delivery [28]. PLGA has been extensively used in formulating many anticancer drugs [20,29,30]. Recently, PLGA has also been used to formulate EVG and tenofovir alafenamide using emulsion solvent evaporation method for prevention of

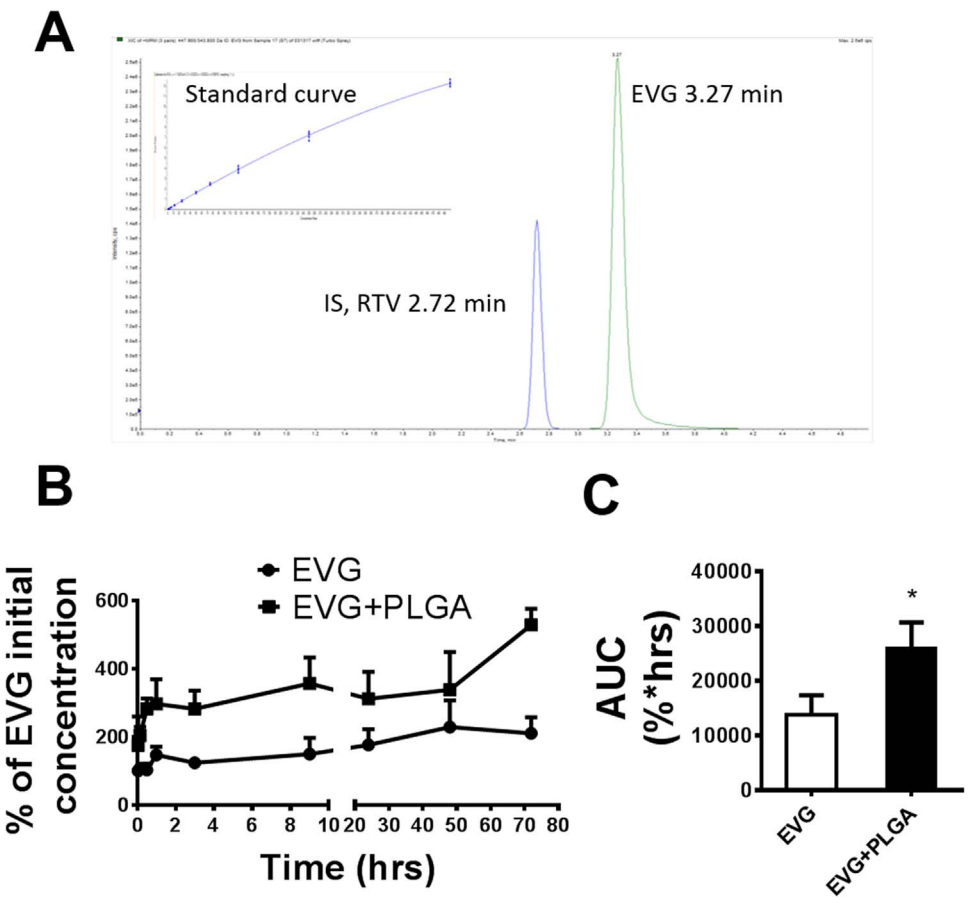

Fig. 3. Intracellular EVG concentration in U1 cells. **A.** LC/MS chromatogram peaks of elvitegravir (EVG) and its corresponding internal standard (IS), ritonavir (RTV) as well as standard curve for EVG measurement. **B.** Concentration time profile of EVG and PLGA-EVG nanoparticles in U1 cells. **C.** Area under the curve of EVG and PLGA-EVG nanoparticles. Mean ± SEM values were graphed from 3 independent experiments. *indicate $p < 0.05$ compared to EVG alone treatment. Mean ± SEM values were graphed from 3 independent experiments.

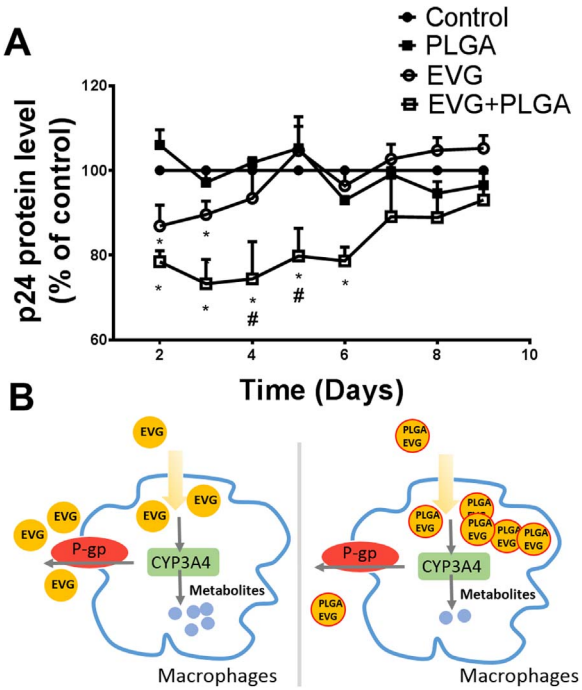

Fig. 4. Viral suppression of PLGA-EVG nanoparticles. **A.** Time course of HIV replication upon drug exposure in HIV-infected monocyte-derived macrophages. Mean ± SEM values were graphed from 3 independent experiments. **B.** A hypothetical mechanism that may explain the higher EVG concentration in PLGA-EVG nanoparticle than EVG alone. *indicate $p < 0.05$ compared to control; #indicate $p < 0.05$ compared to EVG alone treatment. Mean ± SEM values were graphed from 3 independent experiments.

HIV-1 vaginal transmission [31]. The PLGA nanoparticle formation in our study is an oil-in-water (o/w) emulsification, which is an ideal method for water-insoluble drugs [32]. PLGA is the main polymer core to hold EVG molecules; PVA is used to stabilize the emulsion; pluronic polymer F68 is used as a stabilizer and to reverse drug resistance; PLL is used to provide slight positive charge, which helps internalizing into the cells [28,33]. In general, PLGA-based EVG formulation is within the range of 50 nm, and is easy to diffuse through cell membrane to deliver the drugs.

Since HIV replicates within the cells, intracellular drug concentrations are important to determine the efficacy of ART drugs [4]. The intracellular concentrations of ART drugs, especially protease and integrase inhibitors, are dependent on CYP3A4 and P-gp [6,17,25,26,34,35]. These enzymes are highly abundant in the gut and liver, and is the main cause for developing resistance [35]. To enhance the bioavailability of these ART drugs potent inhibitors of CYP3A4 are generally used. Ritonavir and cobicistat are pharmacoenhancers for protease inhibitors and EVG, respectively [36]. We have recently shown the abundance of drug transporters and CYP3A4 in monocytic cells [5,6]. Thus, bypassing transporters and CYP3A4 is considered as an effective strategy to improve the ART drug intracellular concentrations, especially in monocytic cells. Literatures suggest that nanoparticles-based drug delivery would bypass the efflux transporters namely P-gp [37], as well as CYP-mediated liver metabolism [38]. Based on our findings we hypothesize that higher concentration of EVG in PLGA-EVG than EVG alone results from its likely protection from drug transporter P-gp and metabolic enzyme CYP3A4 (Fig. 4B). Our hypothesis is further strengthen from the literature data that the concentration of ART is relatively lower in P-gp- and CYP3A4-expressing monocytic cells than lymphocytic cells [2,5–7]. This PLGA-EVG nanoformulation is also expected to bypass the liver P-gp and CYP3A4.

EVG is usually co-administrated with cobicistat as a

pharmacoenhancer [16,17]. However, co-administration of EVG with cobicistat is relatively expensive. The use of multiple drugs are also likely to cause drug-drug interactions. Thus, developing an optimal EVG formulation without cobicistat can minimize drug dose and subsequent drug-drug interactions. Compared to EVG alone, the EVG nanoformulation can provide a high intracellular drug concentration without pharmacoenhancer, and present relatively increased viral suppression in primary macrophages. In conclusion, this formulation is a step forward to develop EVG nanomedicine that suppresses viral replication at relatively low dose. Our next goal is to develop and optimize EVG nanoformulation that specifically target monocytic cells.

Acknowledgement

We acknowledge Neuroscience Institute, UTHSC, for the use of transmission electron microscopy. We also acknowledge the regional biocontainment laboratory, UTHSC, for providing BSL-3 facility for conducting HIV work. We thank the National Institute of Health for financial support to Santosh Kumar (AA022063 and DA042374) and to Murali M. Yallapu (K22CA174841).

Conflict of interest

None.

Appendix A. Transparency document

Supplementary data associated with this article can be found in the online version at http://dx.doi.org/10.1016/j.bbrep.2017.10.005.

References

[1] K. Kedzierska, S.M. Crowe, The role of monocytes and macrophages in the pathogenesis of HIV-1 infection, Curr. Med. Chem. 9 (2002) 1893–1903.
[2] S. Aquaro, V. Svicher, D. Schols, M. Pollicita, A. Antinori, J. Balzarini, C.F. Perno, Mechanisms underlying activity of antiretroviral drugs in HIV-1-infected macrophages: new therapeutic strategies, J. Leukoc. Biol. 80 (2006) 1103–1110.
[3] A. Kumar, W. Abbas, G. Herbein, HIV-1 latency in monocytes/macrophages, Viruses 6 (2014) 1837–1860.
[4] C. Bazzoli, V. Jullien, C. Le Tiec, E. Rey, F. Mentre, A.M. Taburet, Intracellular pharmacokinetics of antiretroviral drugs in HIV-infected patients, and their correlation with drug action, Clin, Pharmacokinet. 49 (2010) 17–45.
[5] M. Jin, P. Arya, K. Patel, B. Singh, P.S. Silverstein, H.K. Bhat, A. Kumar, S. Kumar, Effect of alcohol on drug efflux protein and drug metabolic enzymes in U937 macrophages, Alcohol Clin. Exp. Res. 35 (2011) 132–139.
[6] T.J. Cory, H. He, L.C. Winchester, S. Kumar, C.V. Fletcher, Alterations in P-glycoprotein expression and function between macrophage subsets, Pharm. Res. 33 (2016) 2713–2721.
[7] C.F. Perno, F.M. Newcomb, D.A. Davis, S. Aquaro, R.W. Humphrey, R. Calio, R. Yarchoan, Relative potency of protease inhibitors in monocytes/macrophages acutely and chronically infected with human immunodeficiency virus, J. Infect. Dis. 178 (1998) 413–422.
[8] W.H. De Jong, P.J.A. Borm, Drug delivery and nanoparticles: applications and hazards, Int. J. Nanomed. 3 (2008) 133–149.
[9] M.M. Yallapu, M. Jaggi, S.C. Chauhan, Curcumin nanoformulations: a future nanomedicine for cancer, Drug Discov. Today 17 (2012) 71–80.
[10] M. Yokoyama, Drug targeting with nano-sized carrier systems, J. Artif. Organs 8 (2005).
[11] S.A. Wickline, A.M. Neubauer, P. Winter, S. Caruthers, G. Lanza, Applications of nanotechnology to atherosclerosis, thrombosis, and vascular biology, Arterioscler. Thromb. Vasc. Biol. 26 (2006) 435.
[12] N.M. Midde, S. Kumar, Development of NanoART for HIV treatment: minding the cytochrome P450 (CYP) enzymes, J. Pers. Nanomed. 1 (2015) 24–32.
[13] S.S. Suri, H. Fenniri, B. Singh, Nanotechnology-based drug delivery systems, J. Occup. Med. Toxicol. 2 (2007) 16.
[14] B.J. Edagwa, T. Zhou, J.M. McMillan, X.M. Liu, H.E. Gendelman, Development of HIV reservoir targeted long acting nanoformulated antiretroviral therapies, Curr. Med. Chem. 21 (2014) 4186–4198.
[15] J.L. Blanco, G. Whitlock, A. Milinkovic, G. Moyle, HIV integrase inhibitors: a new era in the treatment of HIV, Expert Opin. Pharmacother. 16 (2015) 1313–1324.
[16] O.M. Klibanov, Elvitegravir, an oral HIV integrase inhibitor, for the potential treatment of HIV infection, Curr. Opin. Investig. Drugs 10 (2009) 190–200.
[17] N.M. Midde, M.A. Rahman, C. Rathi, J. Li, B. Meibohm, W. Li, S. Kumar, Effect of ethanol on the metabolic characteristics of HIV-1 integrase inhibitor elvitegravir and elvitegravir/cobicistat with CYP3A: an analysis using a newly developed LC-MS/MS method, PLoS One 11 (2016) e0149225.
[18] Y. Pommier, A.A. Johnson, C. Marchand, Integrase inhibitors to treat HIV/Aids, Nat. Rev. Drug Discov. 4 (2005) 236–248.
[19] L.M. Tatham, S.P. Rannard, A. Owen, Nanoformulation strategies for the enhanced oral bioavailability of antiretroviral therapeutics, Ther. Deliv. 6 (2015) 469–490.
[20] M.M. Yallapu, B.K. Gupta, M. Jaggi, S.C. Chauhan, Fabrication of curcumin encapsulated PLGA nanoparticles for improved therapeutic effects in metastatic cancer cells, J. Colloid Interface Sci. 351 (2010) 19–29.
[21] S. Ranjit, N.M. Midde, N. Sinha, B.J. Patters, M.A. Rahman, T.J. Cory, P.S.S. Rao, S. Kumar, Effect of polyaryl hydrocarbons on cytotoxicity in monocytic cells: potential role of cytochromes P450 and oxidative stress pathways, PLoS One 11 (2016) e0163827.
[22] S. Honary, F. Zahir, Effect of zeta potential on the properties of nano-drug delivery systems-a review (Part 1), Trop. J. Pharm. Res. 12 (2013) 255–264.
[23] M.M. Yallapu, S.F. Othman, E.T. Curtis, N.A. Bauer, N. Chauhan, D. Kumar, M. Jaggi, S.C. Chauhan, Curcumin-loaded magnetic nanoparticles for breast cancer therapeutics and imaging applications, Int. J. Nanomed. 7 (2012) 1761–1779.
[24] N. Pirooznia, S. Hasannia, A.S. Lotfi, M. Ghanei, Encapsulation of Alpha-1 antitrypsin in PLGA nanoparticles: In vitro characterization as an effective aerosol formulation in pulmonary diseases, J. Nanobiotechnol. 10 (2012) (20-20).
[25] O. Janneh, T. Anwar, C. Jungbauer, S. Kopp, S.H. Khoo, D.J. Back, P. Chiba, P-glycoprotein, multidrug resistance-associated proteins and human organic anion transporting polypeptide influence the intracellular accumulation of atazanavir, Antivir. Ther. 14 (2009) 965–974.
[26] P. Iyidogan, K.S. Anderson, Current perspectives on HIV-1 antiretroviral drug resistance, Viruses 6 (2014) 4095–4139.
[27] K.K. Pandey, Critical appraisal of elvitegravir in the treatment of HIV-1/AIDS, HIV/AIDS (Auckland, N.Z.) 6 (2014) 81–90.
[28] J.-M. Lü, X. Wang, C. Marin-Muller, H. Wang, P.H. Lin, Q. Yao, C. Chen, Current advances in research and clinical applications of PLGA-based nanotechnology, Expert Rev. Mol. Diagn. 9 (2009) 325–341.
[29] S. Khan, N. Chauhan, M.M. Yallapu, M.C. Ebeling, S. Balakrishna, R.T. Ellis, P.A. Thompson, P. Balabathula, S.W. Behrman, N. Zafar, M.M. Singh, F.T. Halaweish, M. Jaggi, S.C. Chauhan, Nanoparticle formulation of ormeloxifene for pancreatic cancer, Biomaterials 53 (2015) 731–743.
[30] M.S. Zaman, N. Chauhan, M.M. Yallapu, R.K. Gara, D.M. Maher, S. Kumari, M. Sikander, S. Khan, N. Zafar, M. Jaggi, S.C. Chauhan, Curcumin nanoformulation for cervical cancer treatment, Sci. Rep. 6 (2016) 20051.
[31] S. Mandal, P.K. Prathipati, G. Kang, Y. Zhou, Z. Yuan, W. Fan, Q. Li, C.J. Destache, Tenofovir alafenamide and elvitegravir loaded nanoparticles for long-acting prevention of HIV-1 vaginal transmission, AIDS 31 (2017) 469–476.
[32] R.A. Jain, The manufacturing techniques of various drug loaded biodegradable poly (lactide-co-glycolide) (PLGA) devices, Biomaterials 21 (2000) 2475–2490.
[33] A.A. Abdelbary, A.M. Al-mahallawi, M.E. Abdelrahim, A.M.A. Ali, Preparation, optimization, and in vitro simulated inhalation delivery of carvedilol nanoparticles loaded on a coarse carrier intended for pulmonary administration, Int. J. Nanomed. 10 (2015) 6339–6353.
[34] O. Turriziani, N. Gianotti, F. Falasca, A. Boni, A.R. Vestri, A. Zoccoli, A. Lazzarin, G. Antonelli, Expression levels of MDR1, MRP1, MRP4, and MRP5 in peripheral blood mononuclear cells from HIV infected patients failing antiretroviral therapy, J. Med. Virol. 80 (2008) 766–771.
[35] J.C. Kolars, K.S. Lown, P. Schmiedlin-Ren, M. Ghosh, C. Fang, S.A. Wrighton, R.M. Merion, P.B. Watkins, CYP3A gene expression in human gut epithelium, Pharmacogenetics Genom. 4 (1994) 247–259.
[36] M. Vermeir, S. Lachau-Durand, G. Mannens, F. Cuyckens, B. van Hoof, A. Raoof, Absorption, metabolism, and excretion of darunavir, a new protease inhibitor, administered alone and with low-dose ritonavir in healthy subjects, Drug Metab. Dispos. 37 (2009) 809–820.
[37] J. Tang, H. Ji, J. Ren, M. Li, N. Zheng, L. Wu, Solid lipid nanoparticles with TPGS and Brij 78: a co-delivery vehicle of curcumin and piperine for reversing P-glycoprotein-mediated multidrug resistance in vitro, Oncol. Lett. 13 (2017) 389–395.
[38] G. Joshi, A. Kumar, K. Sawant, Bioavailability enhancement, Caco-2 cells uptake and intestinal transport of orally administered lopinavir-loaded PLGA nanoparticles, Drug Deliv. 23 (2016) 3492–3504.